




Article

Investigation of the Behaviour of Steel-Concrete-Steel Sandwich Slabs with Bi-Directional Corrugated-Strip Connectors

Mansour Ghalehnovi ¹, Mehdi Yousefi ^{2,*}, Arash Karimipour ³, Jorge de Brito ^{4,*} and Mahdi Norooziyan ¹

¹ Department of Civil Engineering, Faculty of Engineering, Ferdowsi University of Mashhad, Mashhad 91779-48974, Iran; Ghalehnovi@um.ac.ir (M.G.); mahdi.norooziyan68@gmail.com (M.N.)

² Department of Civil Engineering, Faculty of Maritime Engineering, Chabahar Maritime University, Chabahar 99717-56499, Iran

³ Department of Civil Engineering, University of Texas at El Paso and the Member of Centre for Transportation Infrastructure System, El Paso, TX 79902, USA; akarimipour@miners.utep.edu

⁴ Department of Civil Engineering, Architecture and Georresources, Instituto Superior Técnico, Universidade de Lisboa, 1649-004 Lisbon, Portugal

* Correspondence: m_yousefi@cmu.ac.ir (M.Y.); jb@civil.ist.utl.pt (J.d.B.)

Received: 10 November 2020; Accepted: 30 November 2020; Published: 3 December 2020



Abstract: The most researches on steel-concrete-steel (SCS) sandwich slabs are to control the cracking of concrete core along with losing weight, and shear connector type. In this study, the behaviour of SCS slabs with bi-directional corrugated-strip shear connectors (CSC) was investigated. One of the most important practical problems of CSCs in SCS slabs is lack of access for another end welding to the second steel faceplate. In this research, plug weld was proposed to provide partial welding of the other end of CSCs to a steel plate. For this reason, three slabs were manufactured using the normal concrete core as a control sample and lightweight concrete (LWC) core with and without steel fibres. The behaviour of these slabs was compared with the behaviour of SCS slabs with J-hook and stud bolt connectors from previous researches. The specimens were tested under a concentrated block load as quasi-statically. Based on the load-displacement relationship at the centre, failure modes, loading capacity, energy absorption, and ductility showed acceptable behaviour for CSC system slabs. There was also a good agreement between the ultimate flexural strength based on experiments and previous research relationships.

Keywords: corrugated-strip connectors; loading capacity; failure modes; energy absorption; ductility

1. Introduction

In order to increase the ratio of strength to weight of the structures and increase energy absorption, in recent years, the combination of concrete with steel faceplates has been considered by researchers. In this combination, a concrete piece can be mounted on a steel faceplate using a sufficient number of shear connectors [1], or a concrete core can be sandwiched between two steel faceplates, which is known as a steel-concrete-steel (SCS) sandwich.

SCS sandwich slabs are made of a concrete core between two steel faceplates connected using adhesive materials or mechanical shear connectors [2,3]. SCS sandwich slabs show better performance in terms of stiffness, strength, and against fire and impact compared to the reinforced concrete slabs manufactured with normal concrete. Using the SCS structure reduces the number of stiffeners and welding processes, for example, in ship-hull. The main advantages of SCS include: (1) the steel faceplates play an important role to increase the flexural behaviour and construction efficiency,

(2) the steel plates increase the impact resistance of concrete slab, and (3) also these can act as an impermeable layer, especially for gas and liquid vessels. According to the previous researches, SCSs have excellent structural performance in terms of static, impact, and blast strength [4–7]. SCSs can be used in different projects, including submerged tube tunnels, building core walls, offshore structures, bridge decks, etc. [8–11]. In many studies, the SCS has been used to manufacture offshore structural walls for increasing resistance against contact with water floating ice pressures [12,13]. Extensive works have also been done by researchers to investigate the potential use of this system in lightweight deck structures and for the strengthening of weakened areas in ship structures [14,15]. To improve the composite behaviour of the SCS system, different mechanical shear connectors are developed in two ways of one end welded and two ends welded. The common one end welded shear connectors are C-shaped connectors, as shown in Figure 1a [16], L-shaped connectors, as shown in Figure 1b [3], and overlapped headed studs in a double-skin composite structure (DSC) as illustrated in Figure 1c [17]. One of the drawbacks of these shear connectors used for SCS sandwich construction is their relatively poor performance under high shear force. Additionally, friction welding connectors in Bi-steel structure [18] and J-hook connectors [19–22] are the common two end welded shear connectors, as demonstrated in Figure 1d,e, respectively. Bi-steel connectors are the best in comparison to other shear connectors in terms of performance but with two serious practical problems including, (1) Need for advanced friction welding equipment, and (2) Minimum height at least 200 mm for friction welding. The SCS construction with J-hook shear connectors does not have Bi-steel problems due to interlocking J-hook connectors after preparing each faceplate with one end welded shear connectors. However, precisely adjust the hooks against each other, and straightening hooks under loading can be the drawbacks of the J-hook connectors. There is limited literature on the development of corrugated-strip connectors (CSC) (Figure 1f) that were first proposed by Leekitwattana et al. in 2010 [2,23]. One of the advantages of this system compared to other shear connectors is that unlike previous models in which shear connectors are normal to steel face plates, the angle of shear connectors can be aligned perpendicular to the diagonal crack line of concrete approximately. In this system, shear connectors are welded to steel face plates from both sides that create thickness limitation in practice and need modern welding equipment to connect both sides of connectors to both steel face plates similar to Bi-steel system. Practical restrictions can be the main reason for the non-development of these shear connectors. In this research, practical solutions for the development of the CSC shear connectors are presented in SCS slabs.

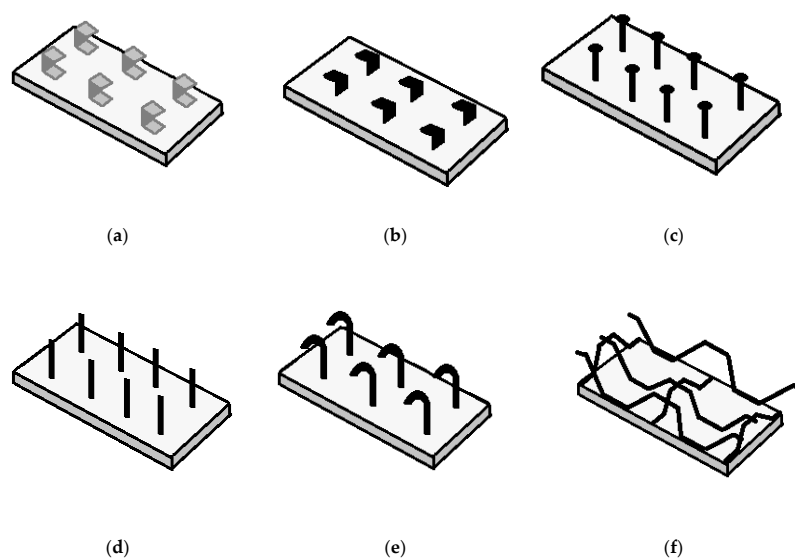


Figure 1. Shear connectors in SCS sandwich structures. (a) C-shaped connectors, (b) L-shaped connectors, (c) overlapped headed studs in DSC system, (d) friction welding connectors in Bi-steel structure, (e) J-hook connectors, (f). corrugated-strip connectors (CSC).

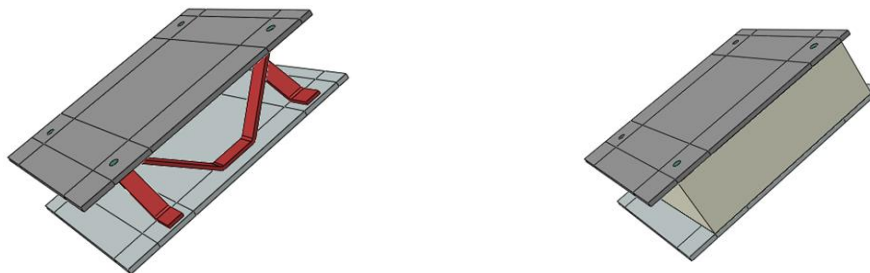
Many types of research have been done on the performance of SCS sandwich members. In 2011, Sohel and Liew [24] studied eight SCS slabs which consist of a lightweight concrete core sandwiched in between two steel plates interconnected by J-hook connectors under concentrate static load. The maximum resistance of the SCS slabs was governed by either the flexural resistance of the slab or punching shear resistance of the concrete core. After that, in 2014, Sohel and Liew [25] evaluated the behaviour of J-hook SCS sandwich slabs with lightweight concrete core subject to impact load. Impact tests were carried out using an instrumented drop weight machine. Test data such as deflection- and impact force-time history and permanent deformation after impact were reported. Test observation showed that J-hook connectors provide an effective means to interlock the top and bottom steel faceplates, preventing them from separation upon impact. Steel fibres were added into the concrete core of selected test specimens to evaluate their effectiveness in reducing the brittleness of concrete due to dynamic loads. In another investigation in 2017, Leng and Song [26] assessed the flexural and shear performance of SCS sandwich slabs under concentrate loads. For this aim, six simply supported slabs with different shear spans, section depths and steel configurations were tested under concentrate loads applied at the centre. After the tests, parts of the steel plates were taken off to observe the crack distribution. The observed modes of failure included flexural yielding and shear punching. The former was initiated by tensile yielding of the bottom steel plate, while the latter was primarily due to punching shear failure of the concrete core. Besides, a theoretical model was developed to predict the resistance of SCS slabs under concentrate loads. In 2019, Zhao et al. [27] investigated the performance of SCS slabs under contact blast loading by experiment and numerical method. For this purpose, three small-scale specimens under contact detonation were tested to obtain the failure modes, mid-span deflection, and dynamic response. Nonlinear 3D finite element models were also established to assess the blast behaviour using Arbitrary-Lagrange-Eulerian (ALE) coupled with Fluid-structure interaction (FSI) algorithm. The results indicated that the failure modes of these slabs were summarized as three types such as type I, type II and type III from both experimental and numerical results. The damaged areas of concrete in slabs were more substantial than that of RC slab. Recently, Yan et al. [28] evaluated the Low-velocity impact performance of curved SCS sandwich slabs with bolt connectors. Experimental outcomes including impact force history, displacement history and permanent deformation were analysed to reveal the influences of concrete core and steel plate thickness as well as shear connectors' spacing on the impact performances of SCS slabs. Meanwhile, three failure types were observed from the nine specimens subjected to impact load. The presence of bolt connectors was proven to be an effective way to prevent the detachment of steel plates from the concrete core. It turned out that concrete core was the central part to dissipate impact energy, followed by a top steel plate and bottom steel plate. Golmohammadi et al. [29] conducted test program to investigate the behaviour of SCS which consist of a normal weight concrete core sandwiched in between two steel plates interconnected by stud bolt shear connectors under concentrate static loading. Nine test samples of SCS slabs are made with stud bolt connectors and are put under concentrated load at the centre of the slab. The observed failure modes included concrete core crack, lower plate slip and upper plate buckling, and stud bolt separation. To study load vs. displacement at the centre and load vs. interlayer slip behaviour, stud bolts diameter and concrete thickness were varied. The results of the tests were compared with the results of sandwich slabs with J-hook connectors [24], and better behaviour was observed. One theoretical model was used to predict the bending strength of the slabs. The results of the theoretical model were consistent with the test results.

Researches on the CSC shear connectors proposed by Leekitwattana et al. [23] have been limited to theoretical studies due to the practical problems of the two end welding, especially in slabs. In 2017 and 2018, Yousefi and Ghalehnovi [30,31] investigated and compared the performance of CSCs for interlayer shear behaviour using Push-out tests in two states of one end welded and two ends welded. The interlayer shear strength of the CSCs in the two ends welded form was approximately twice that of the one end welded. In addition, in two end welded state due to bonding of faceplates, there was no sudden failure, and thus more ductility and energy absorption were provided. Therefore,

they proposed a method to perform the two end welded of CSCs, which could help to make easily in construction site and improve structural performance [32]. In this method, as shown in Figure 2a, in the first step, steel faceplates are accurately measured and lined for the installation of the CSCs and creation of the holes required for plug weld. Plug weld is done by filling the holes with arc welding to connect steel faceplates to the inaccessible end of the CSC connectors. Then, the one end of CSCs is welded on steel faceplates. In the following, in accordance with Figure 2b, the two steel faces are located in the opposite position, so that the other end of the CSCs can be welded to steel faceplates using plug weld. Finally, the space between the two steel faces is filled with concrete materials, as shown in Figure 2c experimental studies of SCS beams interconnected by two ends welded CSCs showed acceptable results in terms of ultimate strength as well as ductility and energy absorption under static load compared with one end welded ones. Research on the behaviour of SCS slabs with two ends welded CSCs can also be important.



(a) Steel faceplates lineation and one end welding of CSCs



(b) Another end welding of CSCs by a plug weld

(c) The SCS system in-filled with concrete

Figure 2. Proposed SCS system interconnected by plug welding of CSCs.

One of the most critical developments in composite sandwiches of SCS is possible to use in structures where light weighting is an important criterion, such as ship-hull. Therefore, in this study, the SCS sandwich slab that consists of lightweight concrete (LWC) core sandwiched in between two steel plates interconnected by proposed two ends welded CSC shear connectors under concentrate quasi-static load is assessed. For this purpose, two SCS slabs manufactured with LWC core and steel fibres reinforced LWC core are investigated and compared with that containing normal weight concrete (NWC) core. For this reason, the failure modes of the slabs and the load-displacement relationship are also measured. Besides, the obtained results are compared to those performed in the previous investigations of the ones of the J-hook SCS system [24] and stud bolt SCS system [29]. For a reasonable comparison, the geometrical characteristics of the specimens and the cross-sectional area of the shear connectors are approximately equivalent to those of the selected reference specimens.

2. Experimental Program

2.1. Sandwich Slab Specimens

To investigate the quasi-static performance of the SCS slabs with the CSC shear connectors under central patch load, specimens were manufactured of three types of the concrete including normal-weight

concrete, lightweight lika concrete and steel fibre reinforced lightweight lika concrete. The constituent materials of this system include concrete core, CSC shear connectors, and steel faceplates.

2.2. Concrete Core Components

To manufacture the SCS slabs, three concrete mix designs are presented in Table 1. To evaluate the compressive and tensile strength of concrete in each SCS specimen, six cylinders with a diameter of 150 mm and a height of 300 mm were manufactured and tested under a hydraulic jack. For each mix, the average compressive and tensile strength of three of those cylinders were evaluated. The tensile and compressive concrete strength has been determined according to ASTM C293-08, BS EN 12390-1, 2 and 3 [33–36]. The obtained outcomes are presented in Table 2. In Tables 1 and 2, SCS, NWC, LWC, and SLWC indicate steel-concrete-steel, normal weight concrete, lightweight lika concrete and steel fibre reinforced lightweight lika concrete, respectively.

Table 1. Concrete mix designs.

Specimens	Water (kg/m ³)	Cement (kg/m ³)	Steel Fibres (kg/m ³)	Light Weight Aggregate (kg/m ³)	Natural Coarse Aggregate (kg/m ³)	Natural Fine Aggregate (kg/m ³)	Water/Cement Ratio
NWC	174	370	-	-	1172	690	0.47
LWC	145	580	-	243	-	742	0.25
SLWC	145	580	12	243	-	742	0.25

Table 2. The concrete strength of the mixes.

Specimens	Average Tensile Stress (MPa)	Tensile Strength Coefficient of Variation	Tensile Strength Distribution Factor	Average Compressive Strength (MPa)	Compressive Strength Coefficient of Variation	Compressive Strength Distribution Factor
SCSNWC	3.75	0.041	0.011	38.50	0.57	0.015
SCSLWC	3.40	0.082	0.034	28.43	0.61	0.021
SCSSLWC	3.30	0.160	0.048	30.33	0.65	0.021

The normal weight aggregates were characterized according to the standards: ASTM C136 [37] for grading size analysis, ASTM C29 [38] for particles dry density, ASTM C127 [39] and ASTM C128 [40] for saturated surface dry density, determination of bulk density and the specific gravity of sand and gravel. In this study, lightweight and normal-weight aggregates were used in the SCS slabs. The used lightweight is illustrated in Figure 3. Furthermore, the physical and chemical properties of both kinds of aggregates are presented in Tables 3 and 4, respectively.



Figure 3. Samples of lightweight lika aggregates.

Table 3. Physical properties of normal weight and lightweight aggregates.

Aggregate Type	Apparent Density (g/cm ³)	Bulk Density (g/cm ³)	Water Absorption (wt%)	Crushing Index (%)	Porosity (%)
Normal weight	2.76	2.65	1.441	31.0	3.88
Light weight	1.40	1.15	1.124	18.3	1.57

Table 4. Chemical properties of natural and lightweight aggregates.

Chemical Composition	Aggregate Type	
	Natural	Lightweight
Ca(CO ₃) (%)	72.2	-
SiO ₂ (%)	27.8	-
Ca Mg(CO ₃) ₂ (%)	-	-
Ca Mg(CO ₃) (%)	-	100
Overall diffraction profile (%)	100	100
Background radiation (%)	22.53	25.12
Diffraction peaks (%)	77.65	74.88
Peak area belonging to selected phases (%)	16.09	47.15
Peak area of phase A (Calcium Carbonate Calcite) (%)	11.14	-
Peak area of phase B (Silicon Oxide) (%)	4.87	-
Peak area of phase A (Calcium Magnesium Carbonate)	-	47.15

To manufacture one of three SCS slabs, steel fibres with two bent ends were used in concrete as illustrated in Figure 4. The elastic modulus, density, the tensile strength, length and diameter of the fibres are 200 GPa, 7610 kg/m³, 809 MPa, 50 mm and 1 mm, respectively. In this study, the steel fibres added to the concrete composition at a volume percentage of 1%.

**Figure 4.** Steel fibres.

2.3. Mechanical Properties of CSC Shear Connectors and Steel Faceplates

In this study, CSC shear connectors were used, as shown in Figure 5. These connectors were used to increase coherence between concrete and steel plates.

**Figure 5.** CSC shear connectors.

To determine the properties of the connectors, a specimen was selected and tested under direct tension, according to ASTM E8M [41]. The obtained results are presented in Table 5. Furthermore, the geometric properties of directional corrugated connectors are shown in Figure 6 and Table 6.

Table 5. Mechanical properties of steel faceplates and CSCs.

	Thickness (mm)	Yield Stress (MPa)	Ultimate Stress (MPa)	Ultimate Strain	E_s (GPa)
Steel face plates	6	285	495	0.23	202
CSCs	4	250	380	0.3	207

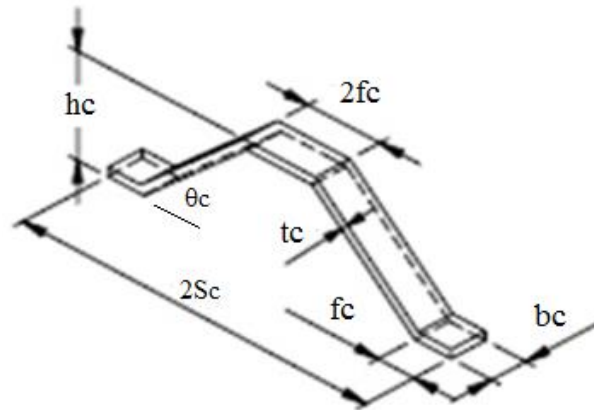


Figure 6. Geometric properties of CSC shear connectors.

Table 6. Dimensional properties of CSC shear connectors.

Sc (mm)	hc (mm)	θ_c (°)	fc (mm)	tc (mm)	bc (mm)
92.7	78.0	61.9	26.6	4.0	20.0

2.4. SCS Slab Specimens Preparing

The specimens were square with 1200 mm side. Additionally, the thickness of the concrete core considered 78 mm. For SCS sandwich beam, it should be ensured that a 45° shear cracking of concrete can be resisted by at least one shear connector. For beams with shallow depth and lightweight concrete core, it is recommended that the spacing of the shear connectors (S_s) should be at least equal to the core thickness to provide effective resistance against shear cracking of concrete core [21]. Therefore, the spacing of the connectors in both directions was assumed constant value of 100 mm for all slab specimens. Specimens conducted under concentrated patch load. The CSC connectors were used to make interlayer shear strength between concrete core and steel plates. The arrangement of holes for welding connectors on the bottom and top plates was different, as described in Table 7. Additionally, the holes in the plates were created by using CNC machines, as shown in Figure 7, and the CSC connectors welding arrangement were performed according to Figure 8a,b. After the welding operation, concreting was performed, and finally, after curing the concrete cores, the specimens were stained with white and prepared for testing, as shown in Figure 9.

Table 7. The arrangement of holes and connectors.

Plate	Number of Holes	The Diameter of the Holes (mm)	Number of Connectors	CSCs Spacing (mm)
top	104	12	52	91
bottom	88	12	44	91

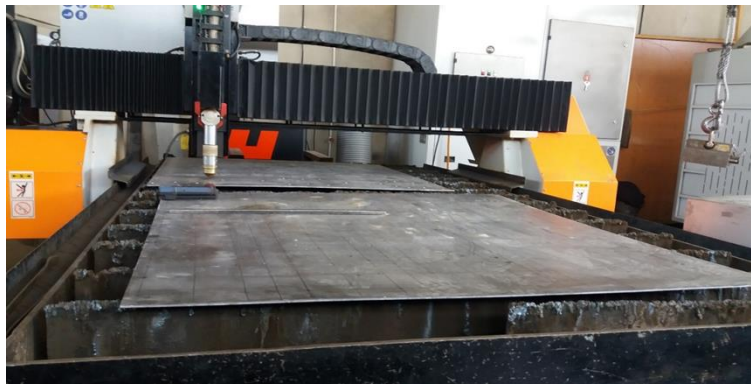


Figure 7. Creating holes in plates using CNC machines.



(a) Line welding for the one end of CSCs



(b) Plug welding for the other end of CSCs

Figure 8. The CSC connectors welding on the steel face plates.



(a) Concrete moulding



(b) Concreting, curing and staining with white

Figure 9. Prepared SCS slabs.

2.5. Required Equipment for Quasi-Static Concentrated Loading Test on SCS Slabs

Specimens were prepared to test after concrete curing. The support of the specimens on the four sides were round bars on the rigid steel bases, as illustrated in Figure 10a. The net length of the slab's spans determined 1000 mm. The patch load was applied at the centre of specimens (see Figure 10b). The tests were performed under quasi-static loading. For this reason, in this test, a hydraulic jack was needed for loading. Additionally, a load-cell with a capacity of 500 kN and an accuracy of 1 mm/min, a data recorder and processor were required. The deflection of the SCS slabs was recorded at each load step by using LVDT at the centre (see Figure 10c).



(a) The support of specimens



(b) Test set-up



(c) LVDT at the central point below the specimen

Figure 10. SCS sandwich slab under quasi-static load.

3. Results and Discussion

3.1. Failure Modes and Load-Displacement Curves

Figure 11 shows an overview of the failure modes of the specimens. The slipping between concrete core and steel layers, the buckling of above steel layers, the cracking of concrete core, and separation of the steel layer from the concrete core because of the removal of CSC shear connectors, especially from the place of plug welds, were the most crucial failure modes of the SCS system. Generally, as shown in Figure 12, the trend of the curves includes 3 stages. The first is elastic behaviour, the second is a flexural failure and finally, despite the core crushing, the load increases due to membrane action. An important point in these slabs with CSC connectors is that at the end of the flexural failure and before the membrane activity begins, the diagram drop of punching failure does not occur. This may be because of the excellent distribution of the connectors, so even after flexural failure, there is a good bonding between the core and the steel face plates.



Figure 11. Deformation of the bottom and top plate.

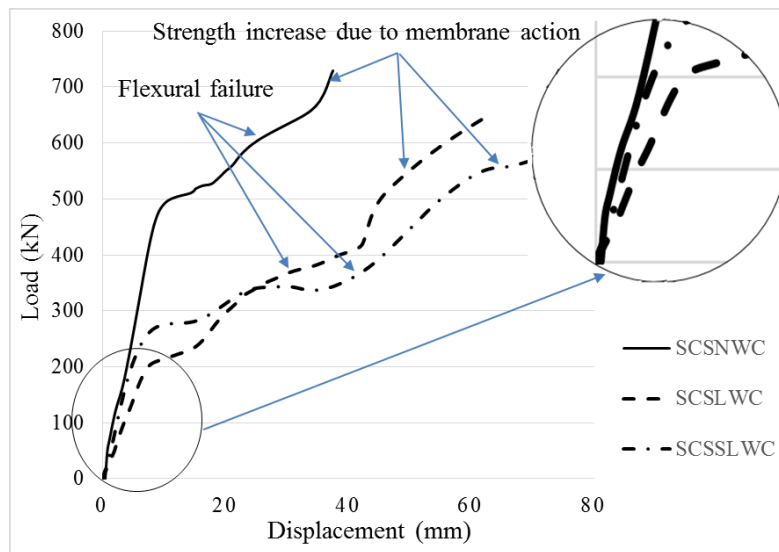


Figure 12. Load-displacement curves of specimens.

One of the main disadvantages of SCS slabs with NWC core is the impossibility of using them in marine structures such as ship-hull due to high weight. So, for this reason, this study was focused on reducing the weight of the SCS slab by using LWC. In Figure 12, the load-displacement curve of the different specimens was shown.

Given the upward trend of the curve even after the onset of membrane activity, it is assumed that the starting point of membrane activity is the ultimate strength of the specimens. According to Figure 12, the typical behaviour of the SCS with NWC core in terms of both stiffness and resistance is better than those produced with plain LWC core and LWC core reinforced by steel fibres. Additionally, the ultimate strength of the specimen with the NWC core is about 670 kN while the ultimate strength of the specimen with LWC core gets roughly two-thirds to around 410 kN; Also, the ultimate flexural strength improves to about 550 kN with using steel fibres. However, the NWC core is about 35% heavier than the LWC and SLWC cores that can be a fundamental problem for specific applications. According to Figure 12, the highest stiffness is for SCS with NWC core, and the least stiffness is for SCS with LWC core. This indicates that the presence of fibres increases both the stiffness and the maximum flexural strength compared to LWC core without steel fibres. In addition, in LWC and SLWC slabs, the connectors acted in less load because of the less compressive strength of LWC than NWC. Figure 13c shows, despite the higher bearing capacity of the SCS with SLWC core, more control over punching has been established than the LWC core. This indicates that the fibres prevent large cracks in the punching area.

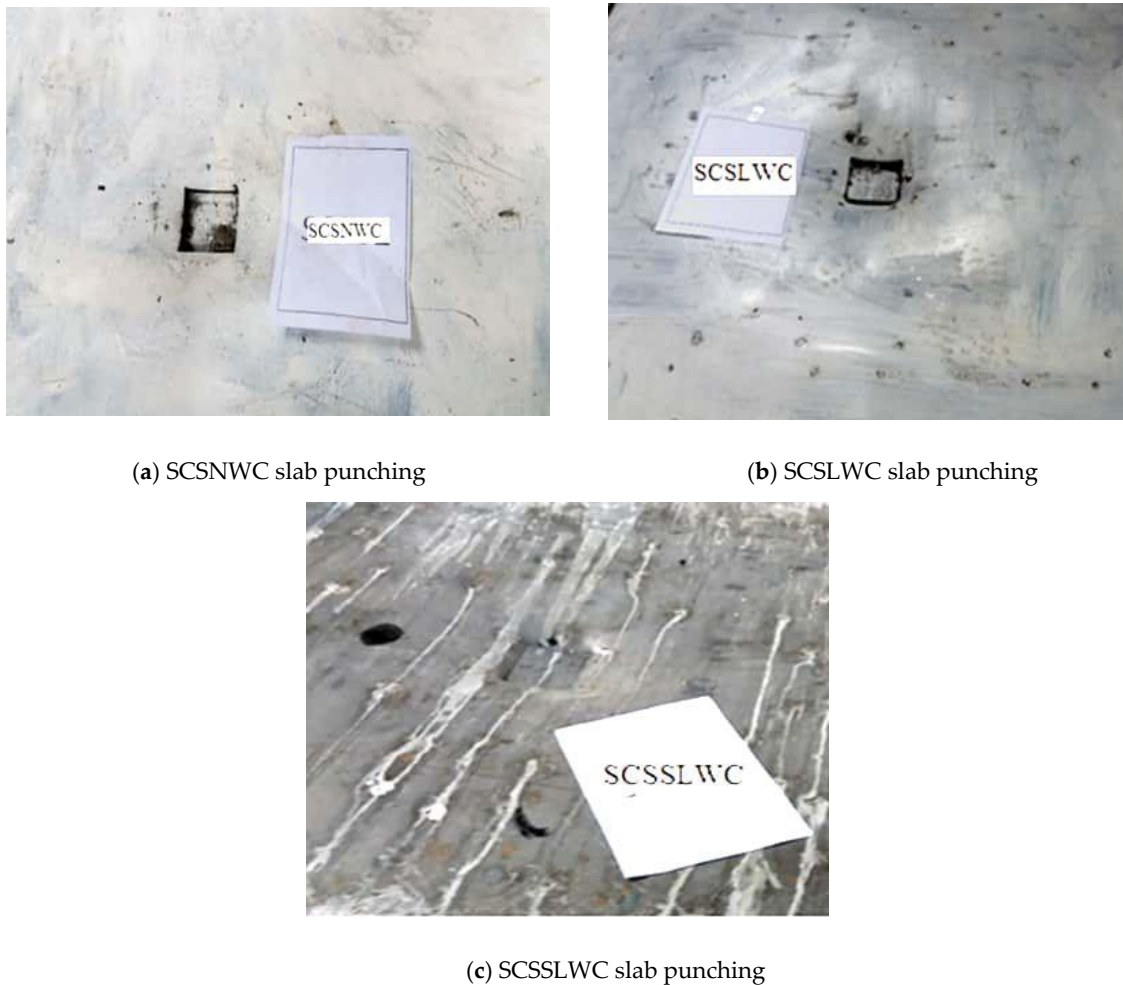


Figure 13. Punching shear failure mode in the specimens.

Besides, the cracks were propagated by increasing the load (Figure 14). As Figure 14a, some of the connectors in the centre of the specimens were detached due to plate slipping and the buckling of the steel face plates. Moreover, the plug weld rupture of the second end of the shear connectors and as a result, the detached CSC connectors was one of the major failure modes of the proposed system. The experiments outcomes showed that in areas where stress concentration was more considerable, the failure of the shear connectors from the plug welds was inevitable; however, this partial joint could significantly improve the shear behaviour of the CSCs compared with the one end welded CSCs studied by Yousefi and Ghalehnavi [30,31]. On the other hand, in the specimen with steel fibres deformation less occurred and the buckling was less in the bottom plate than SCSLWC system (Figure 14b,c) while the buckling occurred in the top plate by increasing load in all specimens.

3.2. Comparison of the Experimental Results with Previous Researches

To show the performance of proposed connectors in this study, the obtained results were compared with other types of connectors, including J-hook [24] and stud bolt connectors [29]. According to Table 8, although, the section area of CSCs is about twice j-hook and stud bolt connectors, this is the least section area that could be used as CSC connector. On the other hand, the number of CSCs for this study is 26% less than ones of J-hook and stud bolt SCS systems. Other specifications are the same except for the specimen SCS6-100, where the strength of NWC core is approximately 48% more than the strength of the NWC core of CSC and stud bolt systems. In addition, the thickness of the concrete core is 100 mm, while other specimens have a thickness of 78 to 80 mm. Besides, it should be noted that, as there is a relation between the modulus of elasticity and the ultimate resistance of the specimens,

the value of E_c for different specimens was also compared, as presented in Table 8. Regarding these results, the modulus of elasticity increased by increasing the compressive strength of the concrete core. Therefore, the maximum load-bearing capacity improved with the increase of the modulus of elasticity (E_c). The obtained outcomes are represented in Figures 15–18. According to Figure 15, in the specimen with J-hook connectors and NWC core, bearing capacity is dropped suddenly after the maximum resistance point of about 600 kN. According to this rapid reduction, failure occurs as a punching shear state. Conversely, using CSC shear connectors leads to increase bearing capacity without any drop in resistant; however, specimens with J-hook connectors deformed more. As it is seen in Figures 16 and 17 with LWC and SLWC core respectively, the reduction after the maximum bearing point of about 250 kN occurs for J-hook connectors due to punching shear failure; however, this sudden drop in resistance is not observed in any of the slabs with CSC connectors. Additionally, compared with those manufactured using stud bolt connectors, CSC connectors resulted in higher bearing capacity of SCS slabs (Figure 18).

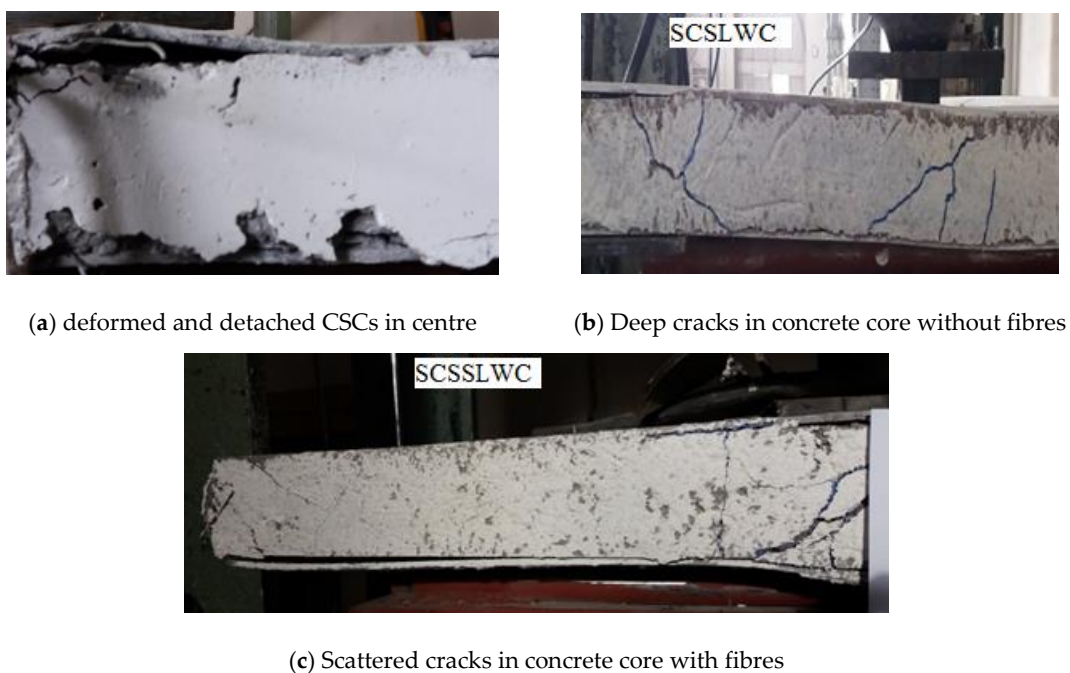


Figure 14. Failure modes of SCS slabs with CSC connectors due to interlayer slipping.

Table 8. Specimens properties of this study and references.

Specimen	A_s (mm ²)	Equivalent Diameter d(eq) (mm)	n_t	h_c (mm)	t (mm)	γ_c (kN/m ³)	f_c (MPa)	E_c (MPa)	σ_y (MPa) for Plates	σ_u (MPa) for Plates
SCSNWC	160	14.3	96	78	6	24.50	38.5	27,377	285	495
SCSLWC	160	14.3	96	78	6	14.30	28.43	24,496	285	495
SCSSLWC	160	14.3	96	78	6	14.50	30.33	25,074	285	495
J-hook NWC SCS6-100 [23]	78	10	121	100	6	24.00	57.2	31,859	315	405
J-hook LWC SLCS6-80 [24]	78	10	121	80	6	14.40	27.0	24,048	315	405
J-hook SLWC SLFCS6-80 [23]	78	10	121	80	6	14.45	28.5	24,518	315	405
SCSB10-1 [29]	78	10	121	80	6	24.00	38.5	27,377	323	560

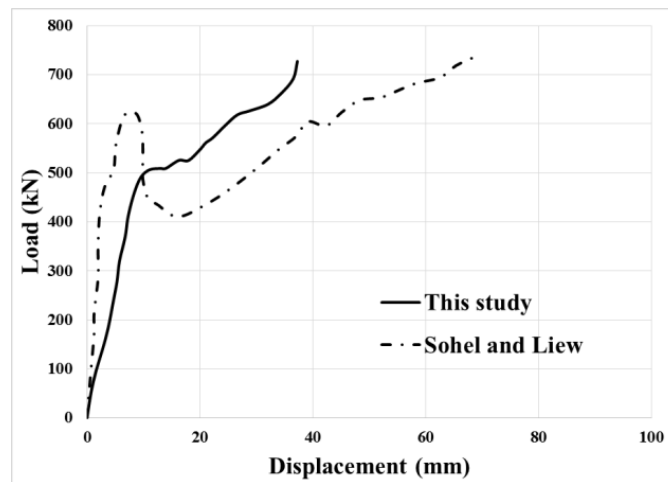


Figure 15. The comparison of the load-displacement curve of SCS slabs with J-hook and CSC connectors with NWC core.

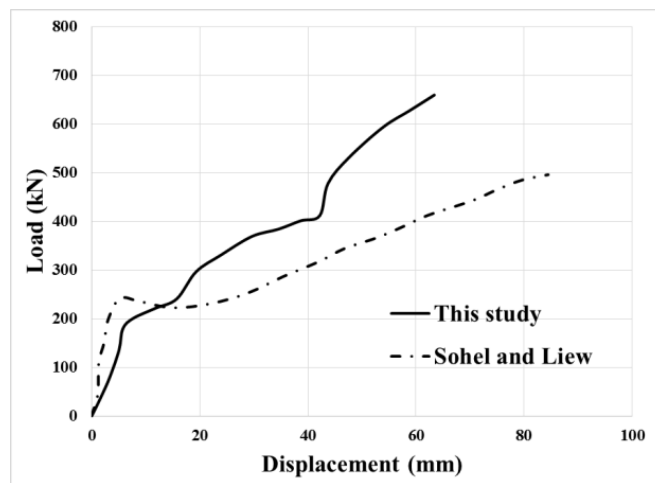


Figure 16. The comparison of the load-displacement curve of SCS slabs with J- hook and CSC connectors with LWC.

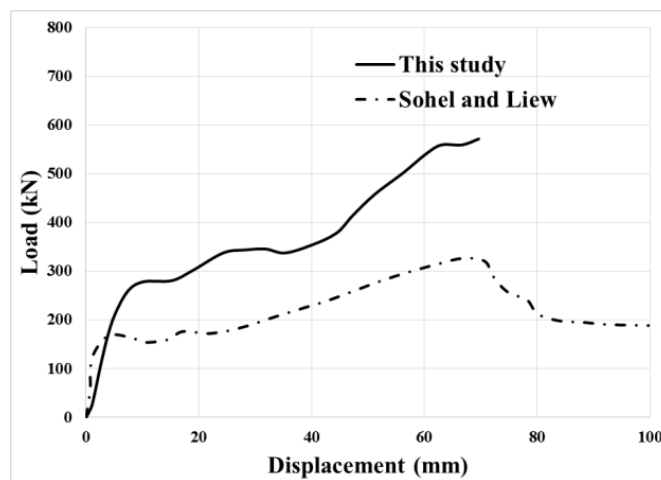


Figure 17. The comparison of the load-displacement curve of SCS slabs with J- hook and CSC connectors with SLWC core.

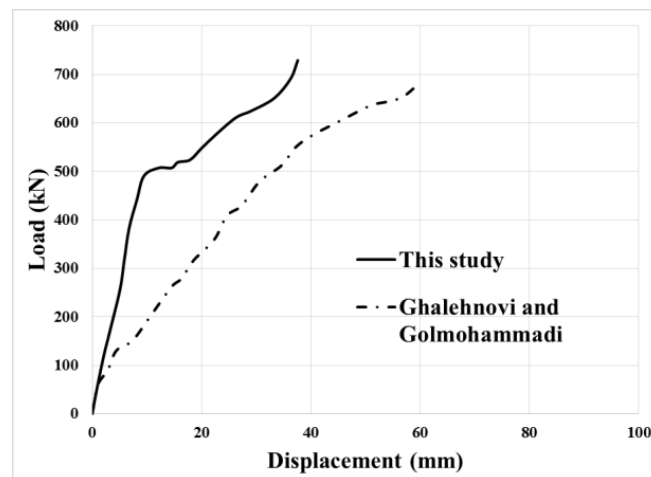


Figure 18. The comparison of the load-displacement curve of SCS slabs with stud bolt and CSC connectors with NWC core.

Stiffness is an essential property and shows the resistance of specimens against the failure. This property is defined as an initial slope of the load-displacement curve of the specimens. So, the stiffness of specimens was measured. Moreover, to assess the structural performance of used connectors, the stiffness of specimens was also compared with that of previous investigation using J-hook and stud bolt connectors, as represented in Figures 15–18 [24,29]. The obtained results of the stiffness of specimens are demonstrated in Figure 19. According to this figure, the stiffness of SCS slabs with CSC connectors proposed in this study are higher than those produced with J-hook connectors by Sohel and Liew [24] and the stud bolt connectors by Ghalehnovi and Golmohammadi [29], except for J-hook system filled by NWC core; however it should be noted that the thickness of the NWC core of the SCS with J-hook connectors is 100 mm, while the thickness of the other samples is about 80 mm.

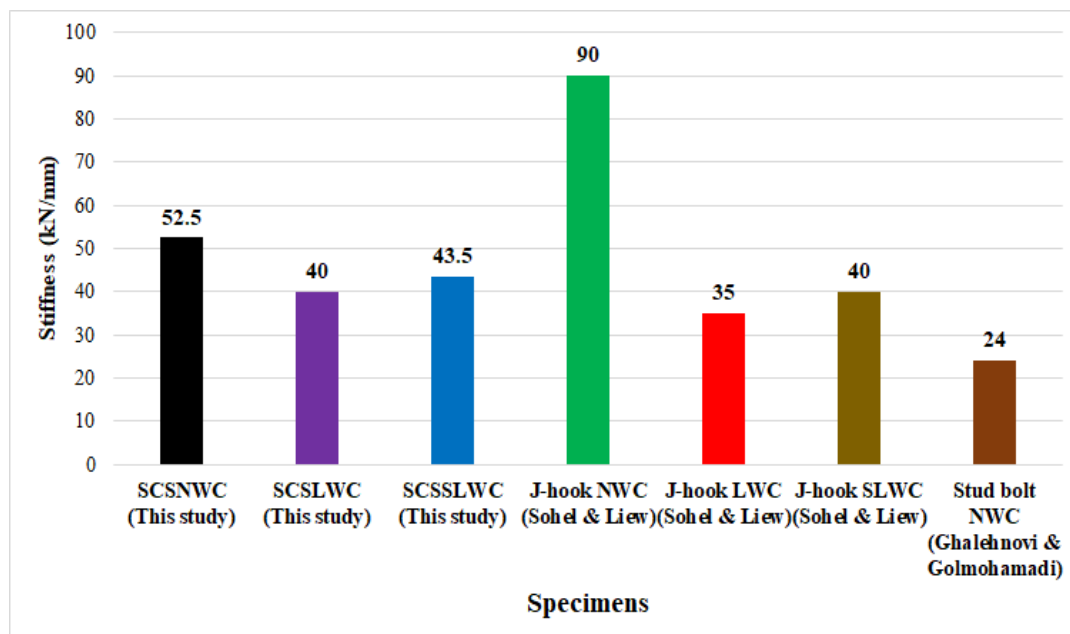
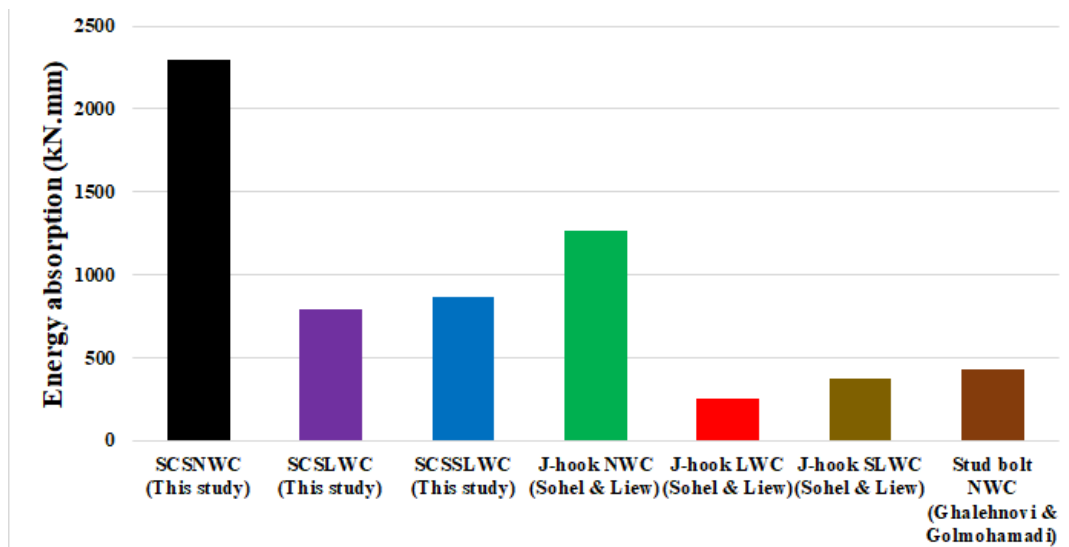


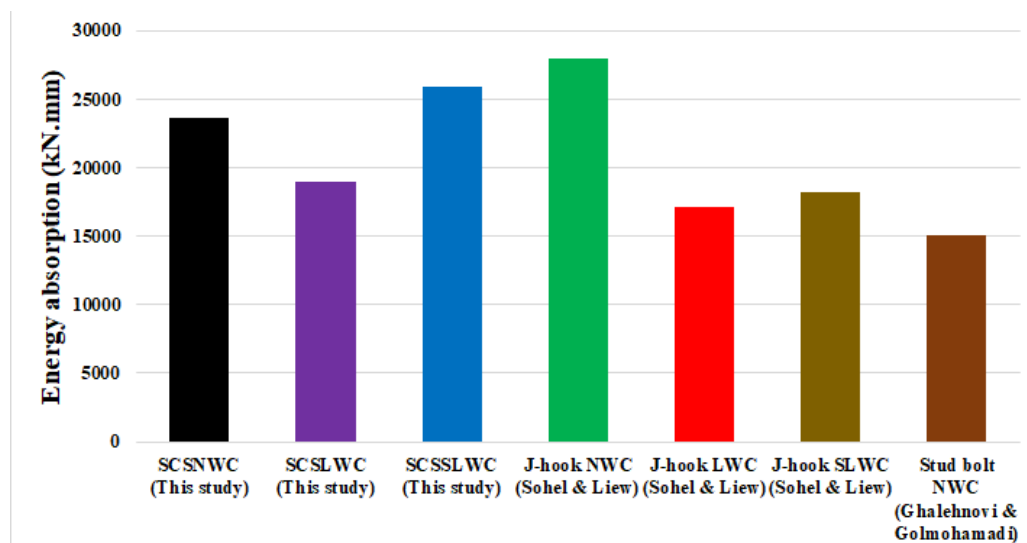
Figure 19. Comparison between the stiffness of the specimens with different types of connectors.

Structures under the external force should have enough potential to compensate the energy resulted from the applied load. For this aim, the energy absorption of the samples under the quasi-static

loading was calculated by the area under curves up to two points of the yield strength and the ultimate bearing capacity. The obtained outcomes are represented in Figure 20 and Table 9.



(a)



(b)

Figure 20. Energy absorption of specimens (a) at the yield strength point and (b) at the ultimate strength.

Table 9. Energy absorption of the specimens.

Specimen	Energy Absorption at the Yield Strength Point (kN mm)	Energy Absorption at the Ultimate Strength (kN mm)
SCSNWC	2299	23,666
SCSLWC	795	18,918
SCSSLWC	864	25,845
J-hook NWC [24]	1262	27,986
J-hook LWC [24]	256	17,149
J-hook SLWC [24]	370	18,158
Stud bolt NWC [29]	430	15,020

According to Table 9 and Figure 20, using LWC has decreased the energy absorption at both yield and ultimate points. Besides, this characteristic at yield and ultimate points was improved when steel fibres was employed approximately 8% and 27%, respectively, compared to LWC core with no steel fibres. Additionally, Figure 20a,b show that up to the yield point the energy absorption of CSC system slabs is substantially more than two other systems, while at the ultimate strength point the difference in energy absorption is significantly reduced for J-hook system slabs. In addition, compared with those produced with stud bolt connectors, using CSC connectors enhances the value of energy absorption at both yield and ultimate strength points, substantially.

For further detail, the ductility ratio of specimens was also evaluated. This index is defined as a ratio of the displacement at ultimate strength (Δ_u) to the displacement related to the yield point (Δ_y) as follows:

$$i = \frac{\Delta_u}{\Delta_y} \quad (1)$$

The obtained results of the ductility of specimens are represented in Table 10. It should be mentioned that in order to show the performance of the proposed connector in this study, the ductility of specimens was compared to those manufactured by J-hook and stud bolt connectors. As it is seen from Table 10, using LWC resulted in raising the ductility ratio, especially when steel fibres were also utilized compared to the ones with NWC core except for NWC core with J-hook connectors. However, this issue will require further studies under the same conditions.

Table 10. Ductility of specimens.

Specimen	i (%)
SCSNWC	4.17
SCSLWC	8.13
SCSSLWC	9.78
J-hook NWC [24]	13.6
J-hook LWC [24]	9.20
J-hook SLWC [24]	10.3
Stud bolt NWC [29]	6.71

3.3. Comparison of the Experimental Strength with the Predicted Strength

In this section, the performance of SCS sandwich slabs containing proposed CSC connectors was compared with the requirements of standards and proposed formulas by other researchers to predict the behaviour of SCS sandwich slabs.

4. Flexural Capacity Prediction of SCS Slabs

Yield-line theory is a method to evaluate the flexural capacity of SCS sandwich slabs. Figure 21 shows a schematic view of the fracture pattern of yield lines in a four edge simply supported slab subjected to a concentrated patch load based on the virtual work principle, the flexural capacity can be calculated using the relation proposed by Rankin and Long [24].

$$F_p = 8m_{pl} \left(\frac{L_s}{L-c} - 0.172 \right) \quad (2)$$

where m_{pl} is the plastic moment capacity per unit length along the yield-line, c is the side length of the loading area, L_s is the dimension of the slab specimens, which here is 1200 mm; L is the span between the supports.

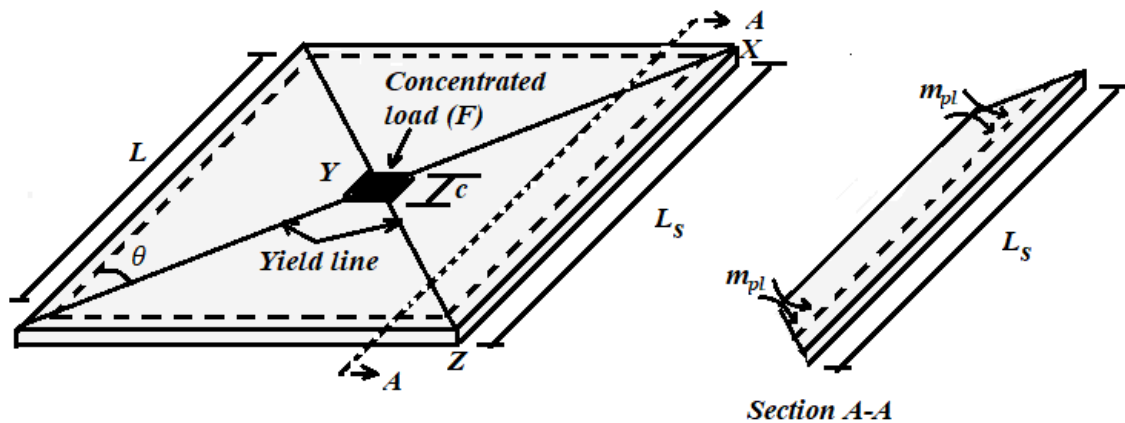


Figure 21. Formation of the yield-line mechanism of SCS slab under concentrated patch load.

The plastic moment resistance of a fully composite SCS sandwich section can be determined by assuming a rectangular plastic stress block of depth x_c for the concrete and the tension and compression stress blocks for the face plates, as shown in Figure 22. The concrete beneath the plastic neutral axis (PNA) is assumed to be cracked. The forces in the steel plates depending on the material yield strength and shear strength of the connectors in resisting interfacial shear stresses between the steel plate and the concrete core. It is also assumed that sufficient shear connectors are provided to prevent local buckling of the compression steel plate [24,29,42].

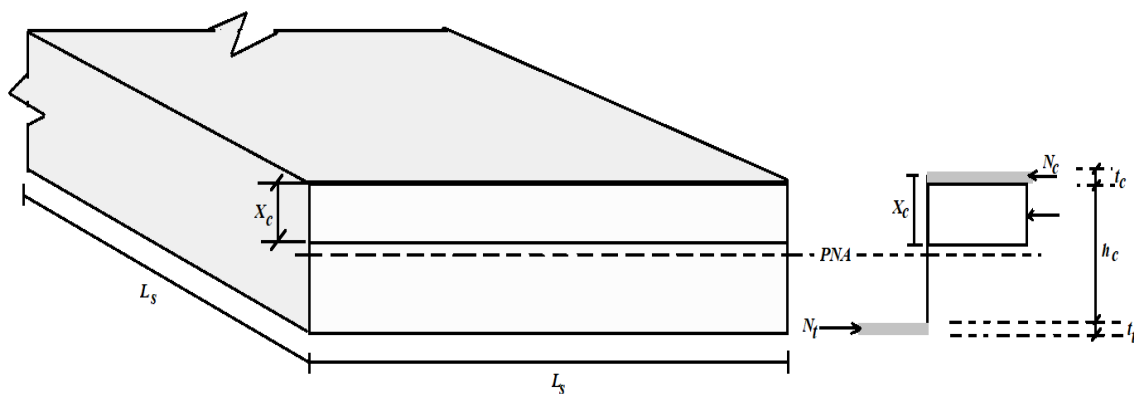


Figure 22. Force distribution in the section at the fully plastic stage.

Since the steel plates are of equal thickness and strength in this particular study, it is assumed $t_c = t_t = t$ in Figure 22. The steel plates in SCS sandwich can be treated as the reinforcement in reinforce concrete. The SCS sandwich slab will deflect extensively and wide cracks are developed in the final loading [8]. After yielding of tension steel plate, the cracking of the concrete will continue to rise towards the compression steel plate. In this case, the strain at the bottom plate is enormous compared to the top steel plate [24]. The moment capacity of the slab is reached when the neutral axis moves near to the lower surface of the compression plate (i.e., $x_c \approx 0$), and the bottom plate is fully yielded. Therefore, in the case of $t_t = t_c = t$, the moment of resistance of the sandwich section becomes [24]:

$$M_{pl} = N_t(h_c + t) \tag{3}$$

For a fully composite member, $N_t = \sigma_y b t_t$, in which σ_y is the yield strength of the steel plate. In this case, it is assumed that the number of shear connectors is sufficient for a fully composite action. Therefore, Equation (3) becomes [24]:

$$M_{pl} = \sigma_y b t_t (h_c + t) \tag{4}$$

In order to achieve a fully composite member, the total number of shear connectors should be $n_s = \sigma_y b t_i / P_R$ in which P_R is the interlayer shear strength of CSC connectors. If full composite cannot be achieved, the member should be designed for partially composite and the moment resistance has to be reduced correspondingly. For partially composite beam,

$$N_t = n_p P_R \tag{5}$$

in which n_p is the actual number of connectors provided between the points of zero and maximum moment. Additionally, P_R for each end of connectors can be obtained by push-out test. However, due to limit push-out test data available, Yousefi and Ghalehnovi [32] proposed a formula to predict P_R as follows:

$$P_R = 16.56 f_c^{0.316} k_{cb}^{-0.79} \theta_r^{-0.3} A_s < 0.8 \sigma_{ult} A_s \tag{6}$$

where f_c is characteristic cylinder strength of concrete; $k_{cb} = \frac{b_c}{b}$ is connector width to connector spacing, θ_r , as shown in Figure 6, is legs angle of connectors (θ_c) in radian and A_s is section area of connectors. Additionally, σ_{ult} is specified tensile strength of CSC but <500 Mpa. According to Table 6, all of CSC connectors have the same geometric properties as follows:

$$k_{cb} = \frac{b_c}{b} = \frac{2}{10} = 0.2; \theta_r = 61.9^\circ = 1.08 \text{ rad}; A_s = 2(20 \times 4) = 160 \text{ mm}^2$$

Also, another formula from the Eurocode 4 [43], offered especially for stud shear connectors of steel-concrete composites, can be compared with Equation (5) approach. This relation is:

$$P_R = 0.29 \alpha d^2 \sqrt{f_c E_c} < 0.8 \sigma_{ult} A_s \tag{7}$$

where E_c is elastic modulus of concrete; d is diameter of stud shear connectors that is equated here based on the area of the rectangular cross section for CSC connectors, $d = \sqrt{4A_s/\pi} = \sqrt{4 \times 160/\pi} = 14.3 \text{ mm}$; f_c is characteristic cylinder strength of concrete; σ_{ult} is ultimate tensile strength of the connector; and A_s is section area of connectors. For CSC connectors, $\alpha = 1$ is assumed as the previous research of Yousefi and Ghalehnovi [30] Therefore, Equation (4) can be written as:

$$M_{pl} = (n_p P_R) (h_c + t) \tag{8}$$

Now consider a square SCS slab containing the n_t CSC shear connectors, as shown in Figure 21. At one-quarter slice (XYZ), the number of CSC connectors in the bottom plate is $n_t/4$. For each yield line in the one-quarter slice, the number of CSC connectors is $n_t/8$. Therefore, the tensile and compressive force in the face plate along the line 'XY' is:

$$N_{t,Rd} = \frac{1}{8} n_t (P_R) \tag{9}$$

therefore, the total flexural capacity of the line 'XY' is written as follows

$$M_{pl} = \frac{1}{8} n_t (P_R) (h_c + t) \leq \sigma_y b t_i (h_c + t) \tag{10}$$

and the flexural moment per unit width along the line 'XY' is

$$m_{pl} = M_{pl}/l \tag{11}$$

where $l = L_s / (2 \cos \theta)$. Substituting Equation (11) into Equation (2), the bearing capacity of the SCS slab (F_p) for the point load can be determined.

5. Comparison of the Results

The comparison between the experimental consequences and those obtained based on the formulas above are represented in Table 11. Table 11 shows that by calculating the P_R based on the Eurocode 4 (Equation (6)), the ultimate flexural strength has a good agreement with under 10% error for all specimens, except for the specimens SCSLWC and SCSB10-1 with 25% and 30% error, respectively. This is also repeated for the proposed relation by Yousefi and Ghalehnovi [32] (Equation (7)) with a good agreement for all CSC systems by below 10% error, exceptionally for SCSLWC specimen that has an unacceptable error of 30%.

Table 11. Comparisons between theoretical predictions and test results of SCS slabs.

Specimen	P_R (kN), Equation (6)	P_R (kN), Equation (7)	m_{pl} , (kN m/m), Equation (6)	m_{pl} (kN m/m), Equation (7)	F_p (kN), Equation (6)	F_p (kN), Equation (7)	F_{p-exp} (kN)	F_{p-exp}/F_{p7}	F_{p-exp}/F_{p7}
SCSNWC	58.5	60.9	69.5	72.3	646	672	670	1.04	1.00
SCSLWC	53.2	49.5	63.2	58.8	587	546	410	0.70	0.75
SCSSLWC	54.3	51.7	64.5	61.4	599	571	550	0.92	0.96
J-hook NWC SCS6-100 [23]	–	33.0	–	62.4	–	579	620	–	1.07
J-hook LWC SLCS6-80 [24]	–	19.0	–	29.1	–	271	252	–	0.93
J-hook SLWC SLFCS6-80 [23]	–	22.3	–	34.2	–	318	302	–	0.95
SCSB10-1 [29]	–	29.8	–	45.6	–	424	550	–	1.30

The results show that the compatibility of the experimental results of the flexural capacity of the beams and slabs with CSC shear connectors and the lightweight concrete core requires future research to obtain an appropriate relationship for the interlayer shear strength (P_R) based on the push-out test [42–47].

6. Conclusions

In this study, the behaviour of SCS sandwich slabs with CSC shear connectors was investigated. For this purpose, three specimens were manufactured and tested. Specimens conducted under quasi-static concentrated load. In all specimens, the thickness of steel plates was the constant and concrete core of slab manufactured with different concrete. Three CSC slabs were manufactured using normal concrete, lightweight lika concrete and steel fibres reinforced lightweight lika concrete. Then, the load-displacement relationship of specimens, ductility, failure modes, maximum bearing capacity and stiffness of specimens were measured. Moreover, in order to show the performance of SCS slabs with proposed CSC connectors, the obtained outcomes were compared with other types of connectors proposed in previous studies. According to the obtained results, the following conclusions can be drawn:

1. The typical behaviour of the SCS with NWC core in terms of both stiffness and resistance was better than those produced with plain LWC core and LWC core reinforced by steel fibres. However, the NWC core was about 35% heavier than the LWC and SLWC cores that can be a fundamental problem for specific applications such as ship hull;
2. The experiments results illustrated that in areas where stress concentration was more significant, the failure of the shear connectors from the plug welds was inevitable;
3. The use of LWC core decreased significantly the energy absorption at both yield and ultimate points compared with NWC core, while this characteristic was improved with steel fibres about 8% and 27%, respectively, compared with LWC with no steel fibres;
4. The use of LWC core with and without fibres significantly increased ductility. This is in contrast to samples with J-hook connectors. However, it is too early to conclude with this limited number of samples and it can be a more detailed study on the subject of future studies;
5. Using steel fibers reduced the punching shear in SCSSLWC by controlling cracks propagation;

6. Except for the SCSLWC slab with LWC core, in the other specimens, the ultimate flexural capacity based on the experiments were in acceptable agreement with the results of the Eurocode 4 (Equation (6)) and the proposed relation by Yousefi and Ghalehnovi [32] (Equation (7)) by below 10% error. It is important to note that the Equation (7) was obtained with the NWC core, and future research is needed to predict the inter-layer shear strength (P_R) for CSC system with LWC core and SLWC core under push-out tests.

Author Contributions: M.G. and J.d.B.; formal analysis, M.G. and M.Y.; investigation, A.K. and M.N.; methodology, A.K. and M.Y.; software, M.G.; supervision, M.Y. and J.d.B.; writing—original draft, A.K. and M.Y.; writing—review and editing, J.d.B. All authors have read and agreed to the published version of the manuscript.

Funding: This research received no external funding.

Acknowledgments: The authors wish to thank the CERIS (Civil Engineering Research and Innovation for Sustainability) research centre and the FCT (Foundation for Science and Technology).

Conflicts of Interest: The authors declare that they have no conflict of interest.

Data Availability: The raw/processed data required to reproduce these findings cannot be shared at this time as the data also forms part of an ongoing study.

Notation

ALE	arbitrary-Lagrange-Eulerian
CSC	corrugated-strip shear connectors
c	side length of the loading area
d	diameter of stud shear connectors
E_c	elastic modulus of concrete
f_c	cylinder strength of concrete
Δ_u	displacement at ultimate strength
Δ_y	displacement related to the yield point
LWC	lightweight concrete
L_s	dimension of the slab specimens
L	span between the supports
m_{pl}	plastic moment capacity per unit length
NWC	normal weight concrete
PNA	plastic neutral axis
P_R	interlayer shear strength of CSC connectors
SCS	steel-concrete-steel
σ_y	yield strength of the steel plate

References

- Meghdadian, M.; Ghalehnovi, M. Improving seismic performance of composite steel plate shear walls containing openings. *J. Build. Eng.* **2019**, *21*, 336–342. [\[CrossRef\]](#)
- Karimipour, A.; Edalati, M. Shear and flexural performance of low, normal and high-strength concrete beams reinforced with longitudinal SMA, GFRP and steel rebars. *Eng. Struct.* **2020**, *21*, 111086. [\[CrossRef\]](#)
- Soty, R.; Shima, H. Formulation for maximum shear force on L-shape shear connector subjected to strut compressive force at splitting crack occurrence in steel-concrete composite structures. *Procedia Eng.* **2011**, *14*, 2420–2428. [\[CrossRef\]](#)
- Wright, H.; Oduyemi, T.; Evans, H. The experimental behaviour of double skin composite elements. *J. Constr. Steel Res.* **1991**, *19*, 97–110. [\[CrossRef\]](#)
- Roberts, T.; Edwards, D.; Narayanan, R. Testing and analysis of steel-concrete-steel sandwich beams. *J. Constr. Steel Res.* **1996**, *38*, 257–279. [\[CrossRef\]](#)
- Karimipour, A.; Edalati, M. Retrofitting of the corroded reinforced concrete columns with CFRP and GFRP fabrics under different corrosion levels. *Eng. Struct.* **2020**, *227*, 145872.
- Dai, X.X.; Liew, J.R. Fatigue performance of lightweight steel-concrete-steel sandwich systems. *J. Constr. Steel Res.* **2010**, *66*, 256–276. [\[CrossRef\]](#)

8. Bowerman, H.; Coyle, N.; Chapman, J. An innovative steel/concrete construction system. *Struct. Eng.* **2002**, *80*, 33–38.
9. Subedi, N.K.; Coyle, N.R. Improving the strength of fully composite steel-concrete-steel beam elements by increased surface roughness—An experimental study. *Eng. Struct.* **2002**, *24*, 1349–1355. [[CrossRef](#)]
10. Zhao, X.L.; Han, L.H. Double skin composite construction. *Prog. Struct. Eng. Mater.* **2006**, *8*, 93–102. [[CrossRef](#)]
11. Xie, M.; Foundoukos, N.; Chapman, J. Static tests on steel-concrete-steel sandwich beams. *J. Constr. Steel Res.* **2007**, *63*, 735–750. [[CrossRef](#)]
12. Bowerman, H.; Chapman, J.C. Bi-steel steel-concrete-steel sandwich construction. *Compos. Constr. Steel Concr.* **2000**, *12*, 656–667.
13. Mohamedien, A.; Omer, A. Finite Elements Modeling and Analysis of Double Skin Composite Plates. *IOSR J. Mech. Civ. Eng.* **2014**, *6*, 254–261. [[CrossRef](#)]
14. Karimipour, A.; Ghalehnovi, M.; de Brito, J.; Attari, M. The effect of polypropylene fibres on the compressive strength, impact and heat resistance of self-compacting concrete. *Structures* **2020**, *25*, 72–87. [[CrossRef](#)]
15. Ghalehnovi, M.; Karimipour, A.; de Brito, J. Influence of steel fibres on the flexural performance of reinforced concrete beams with lap-spliced bars. *Constr. Build. Mater.* **2019**, *229*, 145264. [[CrossRef](#)]
16. Shariati, M.; Sulong, N.R.; Suhatri, M.; Shariati, A.; Khanouki, M.A.; Sinaei, H. Behaviour of C-shaped angle shear connectors under monotonic and fully reversed cyclic loading: An experimental study. *Mater. Des.* **2012**, *41*, 67–73. [[CrossRef](#)]
17. Karimipour, A.; Ghalehnovi, M. Comparison of the effect of the steel and polypropylene fibres on the flexural behaviour of recycled aggregate concrete beams. *Structures* **2021**, *29*, 129–146. [[CrossRef](#)]
18. Anvari, A.; Ghalehnovi, M.; de Brito, J.; Karimipour, A. Improved bending behaviour of steel fibres recycled aggregate concrete beams with a concrete jacket. *Mag. Concr. Res.* **2019**, *12*, 63–75. [[CrossRef](#)]
19. Yan, J.B.; Liew, J.R.; Zhang, M.H.; Wang, J. Ultimate strength behavior of steel-concrete-steel sandwich beams with ultra-lightweight cement composite, Part 1: Experimental and analytical Study. *Steel Compos. Struct.* **2014**, *17*, 907–927. [[CrossRef](#)]
20. Liew, J.R.; Sohel, K.; Koh, C. Impact tests on steel-concrete-steel sandwich beams with lightweight concrete core. *Eng. Struct.* **2009**, *31*, 2045–2059. [[CrossRef](#)]
21. Liew, J.R.; Sohel, K. Lightweight steel-concrete-steel sandwich system with J-hook connectors. *Eng. Struct.* **2009**, *31*, 1166–1178. [[CrossRef](#)]
22. Yan, J.B.; Liew, J.; Zhang, M.H. Ultimate strength behavior of steel-concrete-steel sandwich beams with ultra-lightweight cement composite, Part 2: Finite element analysis. *Steel Compos. Struct.* **2015**, *18*, 1001–1021. [[CrossRef](#)]
23. Leekitwattana, M.; Boyd, S.; Sheno, R. Evaluation of the transverse shear stiffness of a steel bi-directional corrugated-strip-core sandwich beam. *J. Constr. Steel Res.* **2011**, *67*, 248–254. [[CrossRef](#)]
24. Sohel, K.; Liew, J.R. Steel-Concrete-Steel sandwich slabs with lightweight core—Static performance. *Eng. Struct.* **2011**, *33*, 981–992. [[CrossRef](#)]
25. Sohel, K.; Liew, J.R. Behavior of steel-concrete-steel sandwich slabs subject to impact load. *J. Constr. Steel Res.* **2014**, *100*, 163–175. [[CrossRef](#)]
26. Leng, Y.B.; Song, X.B. Flexural and shear performance of steel-concrete-steel sandwich slabs under concentrate loads. *J. Constr. Steel Res.* **2017**, *134*, 38–52. [[CrossRef](#)]
27. Zhao, C.; Lu, X.; Wang, Q.; Gautam, A.; Wang, J.; Mo, Y. Experimental and numerical investigation of steel-concrete (SC) slabs under contact blast loading. *Eng. Struct.* **2019**, *196*, 109337. [[CrossRef](#)]
28. Yan, C.; Wang, Y.; Zhai, X. Low velocity impact performance of curved steel-concrete-steel sandwich shells with bolt connectors. *Thin-Walled Struct.* **2020**, *150*, 106672. [[CrossRef](#)]
29. Golmohammadi, M.; Ghalehnovi, M.; Yousefi, M. Experimental investigation of steel-concrete-steel slabs with stud bolt connectors subjected to punching loading. *AUT J. Civ. Eng.* **2019**, *3*, 93–106.
30. Yousefi, M.; Ghalehnovi, M. Push-out test on the one end welded corrugated-strip connectors in steel-concrete-steel sandwich structure. *Steel Compos. Struct.* **2017**, *24*, 125–134. [[CrossRef](#)]
31. Yousefi, M.; Ghalehnovi, M. Finite element model for interlayer behavior of double skin steel-concrete-steel sandwich structure with corrugated-strip shear connectors. *Steel Compos. Struct.* **2018**, *27*, 149–158.
32. Yousefi, M.; Ghalehnovi, M. The Effect of Shear Connectors on the Bending Behavior of Steel-Concrete-Steel Sandwich Beams. Ph.D. Thesis, Ferdowsi University of Mashhad, Mashhad, Iran, 2017.

33. BS EN 12390-1: *Testing Hardened Concrete—Part 1: Shape, Dimensions and Other Requirements for Specimens and Moulds*; British Standard Institution: London, UK, 2000.
34. BS EN 12390-2: *Testing Hardened Concrete. Making and Curing Specimens for Strength Tests*; British Standards Institute: London, UK, 2009.
35. BS EN 12390-3: *Testing Hardened Concrete; Part 3: Compressive Strength of Test Specimens*; British Standards Institution: London, UK, 2002.
36. ASTM International Committee C09 on Concrete and Concrete Aggregates. *Standard Test Method for Flexural Strength of Concrete (Using Simple Beam with Center-Point Loading) 1*; ASTM International: West Conshohocken, PA, USA, 2016.
37. ASTM C136 *Standard Test Method for Sieve Analysis of Fine and Coarse Aggregates*; ASTM International: West Conshohocken, PA, USA, 2016.
38. ASTM C29 *Standard Test Method for Bulk Density (“Unit Weight”) and Voids in Aggregate*; American Society for Testing and Materials: West Conshohocken, PA, USA, 2017.
39. ASTM C127-01 *Standard Test Method for Density, Relative Density (Specific Gravity), and Absorption of Coarse Aggregate*; ASTM International: West Conshohocken, PA, USA, 2001.
40. ASTM C128 *Standard Test Method for Density, Relative Density (Specific Gravity), and Absorption of Fine Aggregate*; American Society for Testing and Materials: West Conshohocken, PA, USA, 2012.
41. ASTM E8/E8M-16a *Standard Test Methods for Tension Testing of Metallic Materials*; ASTM International: West Conshohocken, PA, USA, 2001.
42. Ghalehnovi, M.; Karimipour, A.; de Brito, J.; Chaboki, H.R. Crack width and propagation in recycled coarse aggregate concrete beams reinforced with steel fibres. *Appl. Sci.* **2020**, *10*, 7587. [[CrossRef](#)]
43. Rankin, G.; Long, A. Predicting the punching strength of conventional slab-column specimens. *Proc. Inst. Civ. Eng.* **1987**, *82*, 327–346.
44. Johnson, R.P.; Anderson, D. *Designers’ Guide to EN 1994-1-1: Eurocode 4, Design of Composite Steel and Concrete Structures. General Rules and Rules for Buildings, Part 1*; Thomas Telford Ltd.: London, UK, 2004.
45. Karimipour, A. Effect of untreated coal waste as fine and coarse aggregates replacement on the properties of steel and polypropylene fibres reinforced concrete. *Mech. Mater.* **2020**, *150*, 103592. [[CrossRef](#)]
46. Karimipour, A.; Edalati, M. Influence of untreated coal and recycled aggregates on the mechanical properties of green concrete. *J. Clean. Prod.* **2020**, *29*, 124291. [[CrossRef](#)]
47. Karimipour, A.; Ghalehnovi, M.; de Brito, J. Mechanical and durability properties of steel fibre-reinforced rubberised concrete. *Constr. Build. Mater.* **2020**, *257*, 119463. [[CrossRef](#)]

Publisher’s Note: MDPI stays neutral with regard to jurisdictional claims in published maps and institutional affiliations.



© 2020 by the authors. Licensee MDPI, Basel, Switzerland. This article is an open access article distributed under the terms and conditions of the Creative Commons Attribution (CC BY) license (<http://creativecommons.org/licenses/by/4.0/>).